Phosphoinositide–Specific Phospholipase C δ1 Activity toward Micellar Substrates, Inositol 1,2–Cyclic Phosphate, and Other Water–Soluble Substrates: A Sequential Mechanism and Allo…

5 AUTHORS, INCLUDING:

Yiqin Wu
The Scripps Research Institute
25 PUBLICATIONS **1,263** CITATIONS

SEE PROFILE

Roger Williams
University of Cambridge
122 PUBLICATIONS **11,944** CITATIONS

SEE PROFILE

Matilda Katan
University of London
100 PUBLICATIONS **4,687** CITATIONS

SEE PROFILE

Mary F Roberts
Chestnut Hill College
252 PUBLICATIONS **6,217** CITATIONS

SEE PROFILE

Phosphoinositide-Specific Phospholipase C δ1 Activity toward Micellar Substrates, Inositol 1,2-Cyclic Phosphate, and Other Water-Soluble Substrates: A Sequential Mechanism and Allosteric Activation[†]

Yiqin Wu,[‡] Olga Perisic,[§] Roger L. Williams,[§] Matilda Katan,[||] and Mary F. Roberts*,[‡]

Merkert Chemistry Center, Boston College, Chestnut Hill, Massachusetts 02167, MRC Laboratory of Molecular Biology, Hills Road, Cambridge CB2 2QH, U.K., and CRC Centre for Cell and Molecular Biology, Chester Beatty Laboratories, Fulham Road, London SW3 6JB, U.K.

ABSTRACT: The kinetics of full-length and PH domain truncated cloned PI-PLC δ1 from rat toward soluble substrates [inositol 1,2-(cyclic)-phosphate (cIP) and glycerophosphoinositol phosphates (GPIP$_x$)] as well as PI in detergent micelles provide the following insights into the mechanism of this enzyme. (i) That cIP is a substrate for the enzyme implies a two-step mechanism for PI hydrolysis [intramolecular phosphotransferase reaction to form cIP followed by cyclic phosphodiesterase activity to form inositol-1-phosphate (I-1-P)]. The dependence of enzyme activity on cIP is sigmoidal, suggesting a transition between less active and more active forms of the enzyme that is affected by substrate. (ii) Interfaces increase the k_{cat} for cIP (but do not affect the cooperativity), and this allosteric activation requires an intact PH domain. (iii) Phosphorylation of the soluble inositol phosphodiesters GPI, GPIP, and GPIP$_2$ enhances PI-PLC δ1 activity by dramatically increasing k_{cat} and decreasing K_m. For these phosphodiesters, the substrate saturation curve is no longer sigmoidal but hyperbolic, indicating the phosphorylated substrate can shift the enzyme to the activated form. (iv) Given the kinetic parameters for cIP hydrolysis and the constant ratio of cIP/I-1-P generated during PI hydrolysis, the cIP produced *in situ* is either released (and not readily rebound since its concentration is well below K_m) or attacked by a water molecule for the generation of the acyclic product.

Phosphoinositide-specific phospholipase C (EC 3.1.4.11) enzymes play a central role in many signal transduction cascades (Lee & Rhee, 1995; Rhee et al., 1989; Rhee & Choi, 1992). Mammalian PI-PLC[1] hydrolysis of phosphatidylinositol 4,5-bisphosphate (PIP$_2$) generates two second messengers: water-soluble D-*myo*-inositol 1,4,5-trisphosphate (IP$_3$), which elevates the intracellular calcium level, and membrane-associated diacylglycerol (DAG), which activates many protein kinase C isozymes. Three classes of mammalian PI-PLCs with 10 different isozymes have been characterized (β1−β4, γ1−γ2, δ1−δ4). They are all calcium dependent and prefer phosphorylated inositols (Ryu et al., 1987), though to different extents. Bacterial PI-PLC, with little homology to the catalytic portion of the mammalian sequences, exhibits a phosphotransferase activity

that is responsible for the formation of 1,2-cyclic inositol phosphate derivatives and a cyclic phosphodiesterase activity that leads to acyclic inositol phosphates (Volwerk et al., 1990; Bruzik & Tsai, 1994). A comparison of the structure of the bacterial enzyme (Heinz et al., 1995) to PI-PLC δ1 from rat (Essen et al., 1996) shows them both to have imperfect β-barrels with similar placement of catalytic residues. Interestingly, whereas cIP is the initial (and under most circumstances the only) product detected for PI hydrolysis by the bacterial enzymes (Volwerk et al., 1990; Bruzik et al., 1992), mammalian PI-PLCs generate both cyclic and acyclic inositol phosphates simultaneously. The ratio of cyclic to acyclic products, which appears constant during the reaction time course, depends on the isozyme class ($\beta > \delta > \gamma$), substrate (PI > PIP > PIP$_2$), pH, and calcium concentration (Kim et al., 1989). Early interpretations explained this kinetic behavior as a competitive attack of an activated water molecule instead of the inositol 2-hydroxyl group on the bound phosphodiester linkage (Dawson et al., 1971; Kim et al., 1989) to produce both products in parallel. However, this parallel mechanism where cIP is not an intermediate but a product contradicts the observed retention of the configuration at the 1-phosphorus on formation of acyclic inositol phosphates by PI-PLC β1 (Bruzik et al., 1992). Furthermore, substrate analogs lacking the 2-hydroxyl group were shown not to be hydrolyzable by several PI-PLC enzymes (Seitz et al., 1992). Clearly, a critical experiment in understanding the detailed mechanism of mammalian PI-PLC enzymes is to determine the kinetic parameters for cIP hydrolysis.

The activity of bacterial PI-PLC toward cIP is modulated by several factors (Zhou et al., 1997; Wu & Roberts, 1997) that could also explain the difference in mammalian versus bacterial enzyme hydrolysis of PI and cyclic versus acyclic product generation. Bacterial PI-PLC hydrolysis of cIP can be dramatically activated allosterically by the presence of an interface of PC or PE (Zhou et al., 1997). Water-miscible organic solvents such as isopropyl alcohol, dimethylformamide, or dimethyl sulfoxide also activate PI-PLC hydrolysis of cIP by mimicking the polarity of the interface and thereby stabilizing the active form of the enzyme (Wu & Roberts, 1997).

Here we report a kinetic analysis of PI-PLC $\delta 1$ hydrolysis of cIP and other water-soluble substrates (glycerophosphoinositol phosphates). Determining the kinetic parameters for cIP hydrolysis, and exploring how soluble substrate phosphorylation affects these parameters, allows one to better define the mechanism for PI hydrolysis as well. Modulations of water activity were also examined for their effects on hydrolysis of cIP. All of our kinetic observations strongly support a sequential mechanism for PI hydrolysis with the rate of release of cIP from the enzyme comparable to the rate of an activated water attacking the enzyme-bound cIP to form I-1-P. Comparison of activities of the full-length enzyme versus a mutant, $\Delta(1-132)$PI-PLC $\delta 1$, with the PH domain removed also implies that the PH domain participates not only in binding to interfaces but also in allosterically enhancing enzyme activity.

MATERIALS AND METHODS

Chemicals, Enzyme. DiC$_7$PC was obtained from Avanti and used without further purification. iPrOH, DMSO, and other organic solvents were purchased from Aldrich. Triton X-100, crude PI, PIP, GPI, GPIP, GPIP$_2$, and IP$_3$ were all purchased from Sigma. Crude soybean PI (50% PI, purchased from Sigma) was used for the enzymatic generation of D-*myo*-inositol 1,2-cyclic phosphate (cIP) as described previously (Zhou et al., 1997). About 110 mg of pure cIP was obtained from 1.0 g of crude PI. Purification of PI-PLC $\delta 1$ and $\Delta(1-132)$ PI-PLC-$\delta 1$, a catalytically active deletion variant lacking the N-terminal PH domain, was as described previously (Essen et al., 1997).

Preparation of cIP Assay Solutions. The buffer used in all cIP assays was 50 mM Hepes, pH 7.5. A stock solution of cIP (600 mM) was prepared by dissolving cIP in D$_2$O and adjusting the pH to 7.5 using NaOD. The range of cIP concentrations examined was 5−80 mM. A 100 mM diC$_7$-PC stock solution was prepared in D$_2$O; the pH was adjusted to 7.5. In the cIP assays, 8 mM diC$_7$PC (predominantly micelles given the CMC of 1.5 mM) and different amounts of DMSO were used to study the interfacial activation and organic solvent activation of the cyclic phosphodiesterase reaction. Stock solutions of GPIP$_2$, GPIP, GPI, and IP$_3$ were also prepared in D$_2$O with the pH adjusted to 7.5. The calcium concentration was fixed to 0.5 mM unless otherwise indicated. The total volume of each assay solution was fixed to 350 μL.

Preparation of PI Assay Solutions. PI and PIP solubilized in mixed micelles with Triton X-100 were also examined as substrates for PI-PLC $\delta 1$. Triton X-100 was used as the matrix to solubilize PI since it has been shown that (i) the extremely fast micelle exchange kinetics of Triton X-100

ensure that substrate depletion is not a problem (Soltys & Roberts, 1994), (ii) Triton X-100 is relatively noninteractive with Ca^{2+}, and (iii) Triton X-100 micelles did not affect PI-PLC $\delta 1$ hydrolysis of cIP (vide infra); hence, this interfacial matrix was relatively inert in its interactions with PI-PLC $\delta 1$. The buffer used in the PI assays was 50 mM Hepes, pH 7.5. A stock solution of PI (40 mM) was prepared by dissolving PI in D$_2$O containing 80 mM Triton X-100 and incubating the sample in a bath sonicator for a few minutes. The ratio of PIP$_x$/Triton X-100 was maintained at 1:2 (the minimum ratio of detergent to PI needed to solubilize all the phospholipid). The pH of the stock solution was adjusted to 7.5 using NaOD; the stock solution was optically clear. The PI concentration used in the assays was 8 mM unless otherwise indicated; sample volumes were 350 μL. After optimization, the calcium concentration was fixed at 0.5 mM.

^{31}P NMR Assays of PI-PLC $\delta 1$ Activity. ^{31}P NMR parameters were based on those used previously (Volwerk et al., 1990; Zhou et al., 1997). ^{31}P NMR (202.3 MHz) spectra were acquired using a Varian Unity 500 spectrometer with samples in 5 mm tubes, and 5% phosphoric acid was used as an external reference. For all kinetic runs, a control spectrum ($t = 0$ min) was performed prior to the addition of enzyme. The amount of enzyme added to initiate hydrolysis of water-soluble substrates varied between 18 and 160 μg, depending on the substrates used and assay conditions. For PI and PIP hydrolysis, 6 μg and 50 ng of enzyme were used. After the addition of the appropriate amount of PI-PLC, an arrayed experiment was initiated, and the hydrolysis rates were measured from the integrated intensity of the resonance corresponding to the phosphorylated product as a function of incubation time, typically 2−3 h, at 30 °C unless otherwise indicated. At all temperatures except 55 °C, the reaction time course was linear throughout most of the NMR experiment.

Determination of the Energetic Parameters of PI-PLC Kinetics. The temperature dependence of k_{cat} was analyzed according to transition state theory (Eyring, 1935; Fersht, 1985) which relates the rate constant of a reaction to an equilibrium constant between the reactants and the transition state, a transient high-energy species that decays to form product. The activation free energy, $\Delta G^{\ddagger}$, was calculated by $\Delta G^{\ddagger} = -RT \ln (k_{cat}h/k_BT)$, where h, k_B, and R are Planck's, Boltzmann's, and the gas constant, respectively, and k_{cat} (s^{-1}) is the experimentally determined turnover number. The transmission coefficient (Eyring, 1935) is assumed to be unity (Fersht, 1985) and can be ignored. The activation enthalpy, $\Delta H^{\ddagger}$, was calculated from the slope of plotting ln (k_{cat}/T) versus $1/T$, based on the Eyring equation: ln (k_{cat}/T) = ln (k_B/h) + $\Delta S^{\ddagger}/R$ − $\Delta H^{\ddagger}/RT$. The activation entropy, $\Delta S^{\ddagger}$, was estimated from $\Delta S^{\ddagger} = (\Delta H^{\ddagger} - \Delta G^{\ddagger})/T$.

RESULTS

PI-PLC $\delta 1$ Activity toward cIP. If a sequential mechanism of PI hydrolysis for mammalian PI-PLCs is operational, cIP must be a substrate for the enzyme. Thus, we have tested the ability of PI-PLC $\delta 1$ from rat to hydrolyze cIP. All mammalian PI-PLCs are reported to be calcium-dependent. The dependence of enzyme cyclophosphodiesterase activity on Ca^{2+} was examined using a deletion variant of PI-PLC $\delta 1$ without its PH domain, $\Delta(1-132)$ PI-PLC $\delta 1$ (Figure 1). Calcium was absolutely required for cIP hydrolysis; the
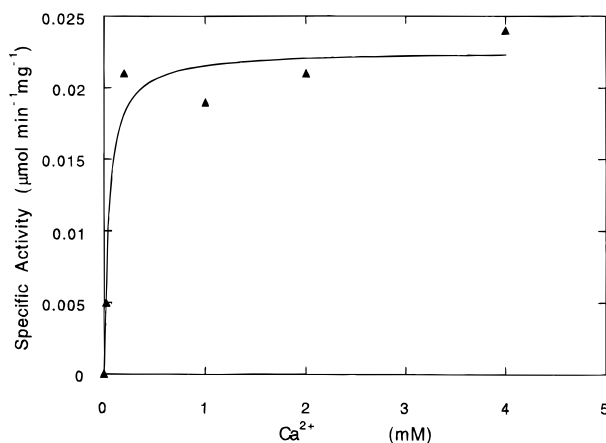
FIGURE 1: Effect of Ca^{2+} concentration on $\Delta(1-132)$ PI-PLC $\delta 1$ cyclic phosphodiesterase activity toward cIP. The curve indicates an apparent K_D of 0.05 ± 0.02 mM. Assay conditions include 50 mM Hepes, pH 7.5, 10 mM cIP, 30 °C, and 60 μg of enzyme.

specific activity of $\Delta(1-132)$ PI-PLC $\delta 1$ toward 5 mM cIP increased in a hyperbolic fashion with added Ca^{2+}. The apparent K_D for metal ion binding at this cIP concentration was 50 μM, a value comparable to what has been determined for PI hydrolysis. Ca^{2+} interacts with the negatively charged PI and cIP species as well as the PI-PLC, so a true K_D and the number of metal ion binding sites cannot be easily extracted from the data. Instead, this Ca^{2+} dependence was used to optimize the assay conditions: 0.5 mM Ca^{2+} was used for all other experiments.

The dependence of enzyme activity on cIP concentration is shown in Figure 2. The curves for cIP hydrolysis in the absence of an interface (indicated by the triangles in both plots) are sigmoidal rather than hyperbolic. The half-saturation concentrations, $[S]_{0.5}$, of cIP are 25 and 28 mM for the $\Delta(1-132)$ PI-PLC $\delta 1$ and full-length enzyme. These values are relatively high. The Hill equation was used to analyze the cooperativity in cIP kinetics. The value for n was 1.7 ± 0.2 and 1.5 ± 0.1 for $\Delta(1-132)$ PI-PLC $\delta 1$ and the full-length PI-PLC, respectively. The V_{max} values determined for truncated and full-length enzymes were essentially identical, 0.40 ± 0.03 and 0.39 ± 0.03 μmol min^{-1} mg^{-1} (Table 1). The K_m values were also similar ($\sim$26 mM). The high values for $[S]_{0.5}$ are unusual in light of the observation that PI hydrolysis yields both cIP and I-1-P products (Kim et al., 1989).

Glycerophosphoinositol Phosphates Are Substrates of PI-PLC $\delta 1$. PI-PLC $\delta 1$ prefers phosphorylated PI molecules as substrates (Ryu et al., 1987; Ellis et al., 1993). This may also be the case for water-soluble substrates. While efficient preparation of cyclic-IP$_x$ is difficult, glycerophosphoinositol phosphates can be used as potential substrates for the enzyme to screen for the effect of adding phosphates to the inositol ring without the complication of different aggregate states of the substrate. They contain the same head group and glycerol backbone as PIP$_x$ without the hydrophobic fatty acyl chains, and they have no tendency to aggregate. Parameters for $\Delta(1-132)$ PI-PLC $\delta 1$ hydrolysis of GPIP$_x$ are summarized in Table 2. A notable comparison is the activity of PI-PLC toward cIP and GPI. The enzyme had a much higher activity toward cIP than toward GPI, probably because the strain energy of cIP (due to the formation of five-member ring) can be released during the hydrolysis of cIP to generate I-1-P (Bruzik et al., 1996). However, adding phosphate to
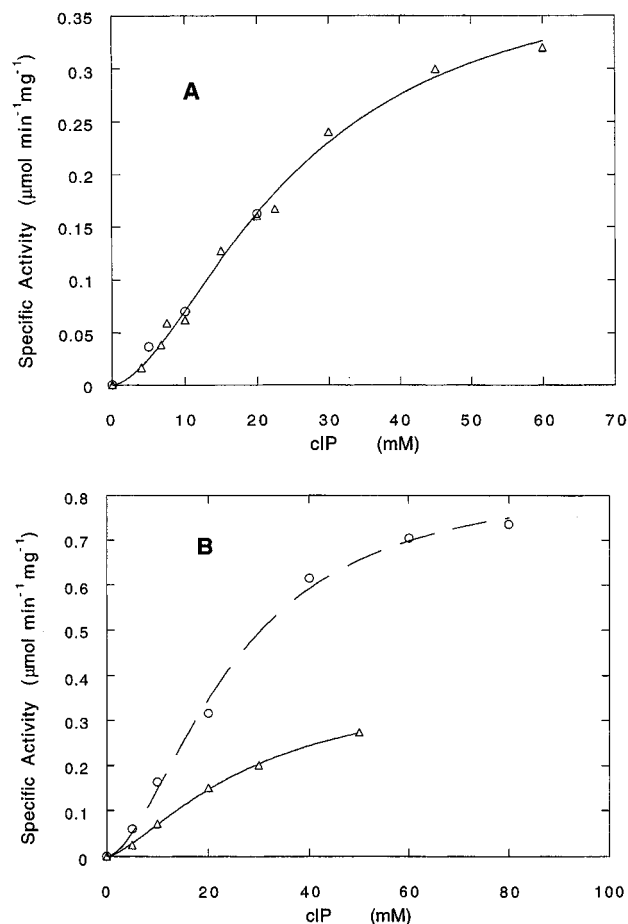

FIGURE 2: Specific activity versus cIP concentration for (A) Δ-$(1-132)$ PI-PLC $\delta 1$ and (B) full-length PI-PLC $\delta 1$ in the absence ($\triangle$) and in the presence ($\bigcirc$) of 8 mM diC$_7$PC. Assay conditions include 50 mM Hepes, pH 7.5, 0.5 mM CaCl$_2$, 30 °C, and 60 μg of enzyme. The curves were drawn by fitting the data with the Hill equation, $V = V_{max}[S]^n/(K_m^n + [S]^n)$, and the parameters are summarized in Table 1.

the inositol ring of GPI generated a substrate that was more efficiently hydrolyzed than cIP. The dependence of GPIP and GPIP$_2$ hydrolysis by $\Delta(1-132)$ PI-PLC $\delta 1$ on substrate concentration was hyperbolic, in contrast to the sigmoidal saturation curves for cIP. The additional phosphates on the inositol ring also made major changes in kinetic parameters. GPIP was a much better substrate (at least 100-fold) than GPI, indicating that the 4'-phosphate of the inositol ring plays an important role in substrate binding and catalysis by PI-PLC $\delta 1$. In comparison with GPIP, GPIP$_2$ showed a 4-fold increase in V_{max} with little change of K_m, indicating that the 5'-phosphate is important for catalysis, but not important for substrate binding. Unlike PI, PIP, and PIP$_2$ hydrolysis by PI-PLC $\delta 1$, which yields both cyclic and acyclic phosphate products (Kim et al., 1989), the hydrolysis of GPI, GPIP, and GPIP$_2$ by PI-PLC $\delta 1$ only produced the acyclic inositol phosphates.

Effect of DiC$_7$PC Micelles on PI-PLC Hydrolysis of cIP. PI-PLC $\delta 1$ as well as the bacterial enzyme were shown to prefer aggregated (micellar) short-chain PI over monomeric PI as substrate (Rebecchi et al., 1993; Lewis et al., 1993). This type of 'interfacial activation' is a characteristic of water-soluble phospholipases hydrolyzing lipophilic substrates. However, another form of interfacial activation was recently reported for the bacterial PI-PLC. PI-PLC from *B. thuringiensis* was activated 21-fold toward cIP (as measured

Table 1: Kinetic Parameters for Hydrolysis of cIP by Δ(1−132) PI-PLC δ1 and Full-Length PI-PLC δ1

assay conditions	Δ(1−132) PI-PLC δ1		full-length PI-PLC δ1	
	V_{max} (μmol min^{-1} mg^{-1})	K_m (mM) (Hill coefficient)[b]	V_{max} (μmol min^{-1} mg^{-1})	K_m (mM) (Hill coefficient)[b]
cIP alone[a]	0.40 ± 0.03	25.2 ± 2.9 (1.7 ± 0.2)	0.39 ± 0.03	28.0 ± 3.0 (1.5 ± 0.1)
+diC$_7$PC (8 mM)	no significant activation observed		0.85 ± 0.06	24.7 ± 2.9 (1.7 ± 0.2)
+45% DMSO	activation curve similar to full-length enzyme		2.0 ± 0.7	30.1 ± 14.2 (1.7 ± 0.5)

[a] Assay conditions include 50 mM, Hepes pH 7.5, 0.5 mM CaCl$_2$, 30 °C. 60 μg of enzyme was added to a total volume of 350 μL of cIP solution to initiate the reaction. [b] Hill coefficient calculated from the Hill equation, $V = V_{max}[S]^n/(K_m{}^n + [S]^n)$.

Table 2: Kinetic Parameters for Hydrolysis of Water-Soluble Phosphodiesters by Δ(1−132) PI-PLC δ1 Hydrolysis[a]

substrate	V_{max} (μmol min^{-1} mg^{-1})	K_m (mM)
GPIP$_2$	4.8 ± 0.6	4.4 ± 1.1
GPIP	0.79 ± 0.08	1.8 ± 0.4
GPI	0.001[b]	
cIP	0.40 ± 0.03	25.2 ± 2.9[c]

[a] Assay conditions include 50 mM Hepes, pH 7.5, 0.5 mM CaCl$_2$, 30 °C. 18, 60, and 120 μg of Δ(1−132) PI-PLC δ1 were used for substrates GPIP$_2$, GPIP, and GPI, respectively. [b] This is the specific activity for 2 mM GPI. [c] This is the K_m value determined from fitting the data with the Hill equation.

by the enzyme efficiency, V_{max}/K_m) by the addition of micellar diC$_7$PC (Zhou et al., 1997). PI-PLC δ1 might also be activated by a PC interface. In the presence of diC$_7$PC micelles (data indicated by the circles in Figure 2), the full-length enzyme exhibited a modest 2-fold increase in V_{max} with little change of K_m; the cooperativity in substrate binding was unaltered (Figure 2B, Table 1). The PC activation was not a general surface activation since Triton X-100 had no effect on the kinetics parameters of the enzyme acting on cIP. In contrast to the results with the full-length enzyme, diC$_7$PC micelles had no effect on Δ(1−132) PI-PLC δ1 hydrolysis of cIP (Figure 2A). This observation suggests that the PI-PLC δ1 PH domain can interact with the PC micelles and in turn alter the catalytic domain conformation in some way that enhances its activity toward cIP.

DMSO Activation of cIP Hydrolysis by PI-PLC δ1. Water-miscible organic solvents have been shown to activate bacterial PI-PLC hydrolysis of cIP by mimicking the interface polarity and inducing a change in the enzyme to a more active form (Wu & Roberts, 1997). The solvent-activated form of bacterial PI-PLC had an increased V_{max} and a dramatically decreased K_m for cIP. DMSO was the most effective of the solvents examined; it lowered the K_m for cIP from 90 mM to about 4 mM (Wu & Roberts, 1997). Since the bacterial PI-PLC and the catalytic domain of the δ1 enzyme show similar structural features, it was of interest to test the mammalian δ1 enzyme for activation by organic solvent. A comparison of the full-length enzyme to Δ(1−132) PI-PLC δ1 might also shed light on the role of the PH domain in the solvent-induced activation. The DMSO activation curves were similar for both Δ(1−132) PI-PLC δ1 and full-length PI-PLC δ1 hydrolysis of 8 mM cIP (Figure 3). The DMSO-induced activation of cIP hydrolysis by PI-PLC δ1 was characterized by a 4−5-fold increase in V_{max} (similar to bacterial PI-PLC) with little change in the [S]$_{0.5}$ or the K_m determined by the fit with the Hill equation (Figure 4, Table 1). If the same data in DMSO were fit with a simple Michaelis−Menten equation, K_m would be 167 ± 160 mM
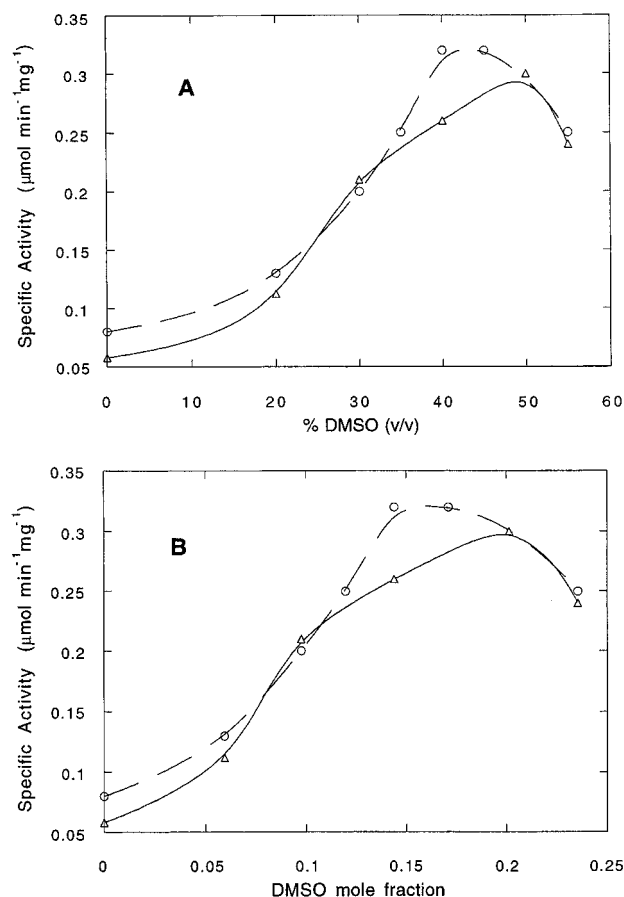

FIGURE 3: Specific activity versus DMSO volume percentage (A) and mole fraction (B) for Δ(1−132) PI-PLC δ1 (△) and full-length PI-PLC δ1 (○). Assay conditions include 50 mM Hepes, pH 7.5, 10 mM cIP, 0.5 mM CaCl$_2$, 30 °C, and 60 μg of enzyme.

with a greater than 80% error in V_{max}. The considerably better fit with a cooperative model (K_m 30 ± 14 mM and 30% error in V_{max}) suggests that solvent activation does not reduce the cooperativity seen for cIP hydrolysis in the absence of additives. The lack of effect on K_m is in striking contrast to the bacterial PI-PLC, where K_m decreased dramatically in the presence of the organic solvent DMSO. Similarly to the bacterial counterpart, the mammalian PI-PLC δ1 activity was sigmoidal as a function of DMSO mole fraction, indicating a cooperative process associated with the addition of DMSO. Besides a possible conformational change associated with the addition of organic solvents which could account for this sigmoidal dependence of activity versus organic solvent mole fraction, another possible explanation for this behavior is the organic solvent dehydration of the PI-PLC active site (Wu & Roberts, 1997). Because the active site of PI-PLC δ1 is broad and solvent-
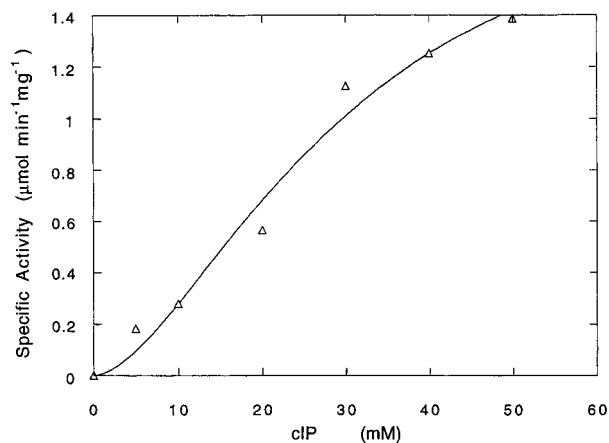
FIGURE 4: Specific activity versus cIP concentration for full-length PI-PLC $\delta 1$ in the presence of 45% DMSO. Assay conditions are the same as in Figure 2. The curve was drawn by fitting the data with the Hill equation, $V = V_{max}[S]^n/(K_m^n + [S]^n)$, and the parameters are summarized in Table 1.

accessible (Essen et al., 1996, 1997), removal of some water may be necessary for productive binding of soluble substrates to PI-PLC. Since many water molecules are involved, the expulsion of active site water could have a cooperative profile and thus give rise to the sigmoidal activity versus organic solvent concentration (Wu & Roberts, 1997).

PIP$_x$ / Triton X-100 Mixed Micelles as Substrates for PI-PLC $\delta 1$. The high $[S]_{0.5}$ (or apparent K_m) for cIP is puzzling in view of the observation that PI hydrolysis by PI-PLC $\delta 1$ yields both cIP and I-1-P. With a K_m of ~25 mM, cIP would be expected as the only product of a simple sequential mechanism for PI hydrolysis under the assay conditions used. The wide range of optimal Ca^{2+} concentrations reported to be needed for PI cleavage (submicromolar to millimolar) presumably reflects differences in the interfaces used in the various assay systems. Amphiphilic PIP$_x$ substrates solubilized in Triton X-100 micelles were used as substrates; mixed micelles of that detergent with phospholipids have been used for kinetic analyses of other phospholipases (Carman et al., 1995). Critical behavior for use of Triton mixed micelles with this PI-PLC is that the Triton X-100 has minimal affinity for Ca^{2+}, rapid micelle exchange kinetics, and does not activate PI-PLC $\delta 1$ toward cIP. The enzyme without the PH domain was used to remove activity differences related to allosteric surface binding. No product was detected if Ca^{2+} was omitted from reaction mixtures containing PI solubilized in Triton X-100 mixed micelles and PI-PLC $\delta 1$. Hydrolysis of PI catalyzed by PI-PLC had a dependence on Ca^{2+} concentration that was similar to cIP hydrolysis (Figure 5). A Ca^{2+} concentration of 0.5 mM was chosen for all assays of PIP$_x$ hydrolysis, as it is sufficiently above the threshold needed for maximum activation of PI-PLC $\delta 1$.

Both the truncated and full-length PI-PLC $\delta 1$ enzymes utilized PI in Triton X-100 micelles as a substrate (Table 3). For 8 mM PI solubilized in 1:2 PI/Triton X-100 mixed micelles, the rates of PI hydrolysis at 30 °C were 16 and 36 μmol min^{-1} mg^{-1} for the truncated and full-length enzymes, respectively. This represented production of both cIP and I-1-P. The ratio of cIP/I-1-P appeared to be constant throughout the reaction. The rates of PI hydrolysis were considerably higher than those for cIP hydrolysis by the same enzymes (which were maximally ~ 1 μmol min^{-1} mg^{-1}). However, these rates were much lower than that for bacterial
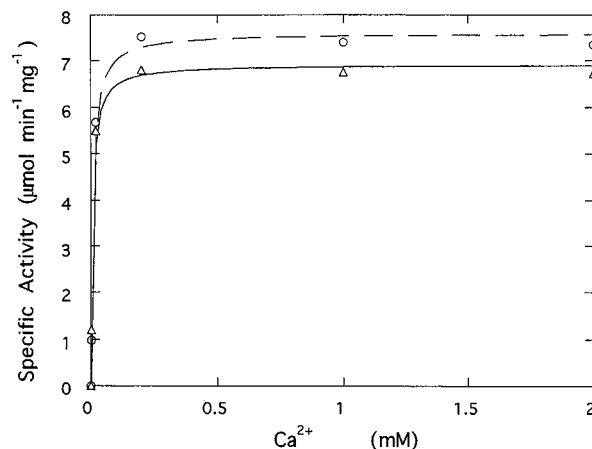

FIGURE 5: Ca^{2+} dependence of $\Delta(1-132)$ PI-PLC $\delta 1$ catalyzed hydrolysis of PI to generate cIP ($\triangle$) and I-1-P ($\bigcirc$). The curve indicates an apparent K_D of 0.008 ± 0.003 mM. Assay conditions included 8 mM PI dispersed in 16 mM TX-100, 50 mM Hepes buffer, pH 7.5, 30 °C, and 6 μg of PI-PLC. The activity was stable at Ca^{2+} concentrations from 0.2 to 30 mM, although the mixture became cloudy above 4 mM Ca^{2+}.

Table 3: Specific Activity for PI-PLC $\delta 1$ Catalyzed Hydrolysis of PI and PIP in TX-100 Micelles[a]

	specific activity (μmol min^{-1} mg^{-1})	
substrate	$\Delta(1-132)$ PI-PLC $\delta 1$	full-length PI-PLC $\delta 1$
PI/TX-100	16	36
PIP/TX-100		
2 mM PIP	1000	
4 mM PIP	1200	

[a] Assay conditions included 50 mM Hepes, pH 7.5, 0.5 mM CaCl$_2$, 30 °C. The ratio of PI or PIP/TX-100 was fixed to 1:2.

PI-PLC hydrolysis of PI in TX-100, which has a V_{max} of 1000 μmol min^{-1} mg^{-1} with an apparent K_m of 1–2 mM (Zhou et al., 1997). Interestingly, the full-length PI-PLC $\delta 1$ was about 2-fold more active than the truncated one for PI hydrolysis. This enhancement was comparable to that observed for cIP hydrolysis by the full-length enzyme in the presence of diC$_7$PC.

Addition of phosphate groups to PI made a much more effective substrate for the enzyme. The truncated enzyme hydrolyzed PIP almost 100 times faster than PI (Table 3), emphasizing that the 4′-phosphate group plays a key role in binding and catalysis. This kinetic activation toward phosphorylated lipophilic substrates is consistent with the observation that enzyme activity was considerably higher toward phosphorylated water-soluble substrates (GPIP or GPIP$_2$ versus GPI or cIP). A kinetic role for the 4′-phosphate was also suggested from the X-ray crystal structure of PI-PLC $\delta 1$ (Essen et al., 1996, 1997). Unlike PI, which when hydrolyzed by PI-PLC is converted to comparable amounts of both cyclic and acyclic phosphate products, PIP hydrolysis by PI-PLC $\delta 1$ produced very little cyclic inositol phosphate (cIP$_2$) and mostly IP$_2$ as the product.

Effect of Solvent Activity on the Ratio of cIP to I-1-P. A curious observation is that PI hydrolysis by PI-PLC $\delta 1$ yielded both cyclic and acyclic inositol phosphates in a relatively fixed ratio. Finding conditions that alter the cIP/I-1-P ratio might help explain why I-1-P is produced at all, given the high K_m for cIP. The generation of I-1-P from cIP involves attack of a water molecule. Thus, a decrease in water activity (a_w) should increase production of cIP. Two
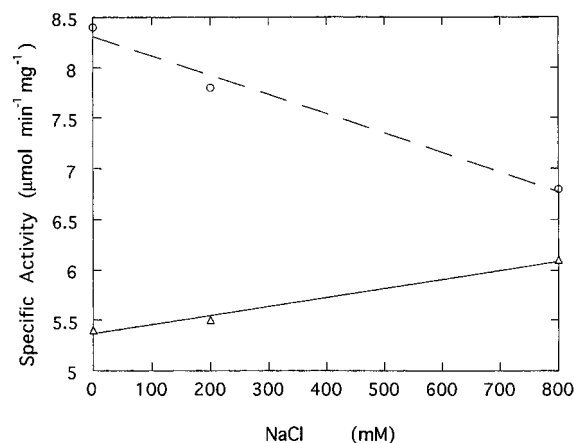
FIGURE 6: Effect of NaCl on $\Delta(1\text{-}132)$ PI-PLC $\delta 1$ catalyzed hydrolysis of PI to generate cIP ($\triangle$) and I-1-P ($\bigcirc$). Assay conditions included 8 mM PI dispersed in 16 mM TX-100, 0.5 mM CaCl$_2$, 50 mM Hepes, pH 7.5, 30 °C. 6 μg of $\Delta(1-132)$ PI-PLC $\delta 1$ was added to the reaction mixture (total volume 350 μL) to initiate the reaction.

Table 4: Effect of Organic Solvent on the Amount of cIP Produced in PI Hydrolysis by PI-PLC $\delta 1$

	cIP (%)	
assay conditions	$\Delta(1-132)$ PI-PLC $\delta 1$	full-length PI-PLC $\delta 1$
standard[a]	46	43
45% DMSO	17	19
25% iPrOH	26	33

[a] Standard assay conditions included 8 mM PI in 16 mM TX-100 mixed micelles, 50 mM Hepes, pH 7.5, 0.5 mM CaCl$_2$.

types of solvent perturbations were used to reduce a_w: addition of (i) NaCl or (ii) water-soluble organic solvents. The effect of moderately high concentrations of NaCl on $\Delta(1-132)$ PI-PLC $\delta 1$ activity toward PI is shown in Figure 6. The overall rate of PI cleavage (I-1-P and cIP production) was almost unaffected from 0 to 800 mM NaCl. However, NaCl slightly increased the rate of cIP production and decreased the rate of I-1-P generation, presumably due to the decreased water activity.

Organic solvents can regulate enzyme activity by changing enzyme conformation (Wu & Roberts, 1997), micelle structure, or water activity (Suzuki & Kanazawa, 1996; Colombo & Bonilla-Rodriguez, 1996). A 2−3-fold activation was observed for the total hydrolysis rate of PI by PI-PLC $\delta 1$ in the presence of 45% DMSO. This amount of solvent did not abolish the PI/TX-100 mixed micelles as monitored by the ^{31}P line width of PI (little change in the PI line width in the presence of these amounts of DMSO). Very interestingly, the presence of 45% DMSO or 25% isopropyl alcohol decreased the cIP/I-1-P ratio significantly (Table 4). NaCl and organic solvents have the opposite effect on the ratio of cIP/I-1-P. The increase in the rate of I-1-P formation caused by organic solvent is not due to the rebinding and hydrolysis of free cIP, because in the assay conditions used the concentration of cIP was well below its K_m.

Effect of Temperature on the Ratio of cIP to I-1-P. One possible explanation for I-1-P production upon PI hydrolysis by PI-PLC $\delta 1$ is that cIP generated *in situ* has a slow off rate compared to its attack by a water molecule. Varying the assay temperature might have a substantial effect on such a rate. If the assay solution bulk dielectric constant and the ionic strength remain unchanged, enzyme kinetics usually
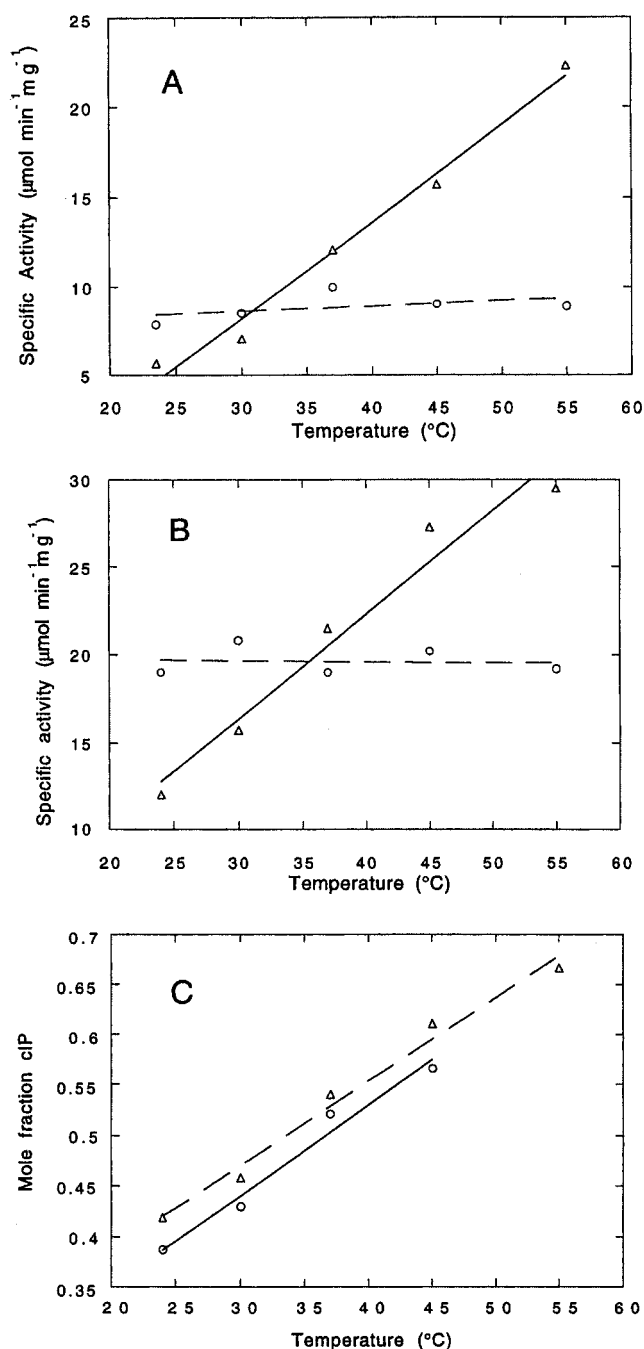
FIGURE 7: Temperature dependence of (A) $\Delta(1-132)$ PI-PLC $\delta 1$ and (B) full-length PI-PLC $\delta 1$ (B) activities toward PI in TX-100 mixed micelles (1:2 PI/Triton X-100): ($\triangle$) generation of cIP; ($\bigcirc$) generation of I-1-P. In (C), the ratio of cIP to I-1-P for the hydrolysis of PI in TX-100 micelles is shown as a function of assay temperature: ($\triangle$) $\Delta(1-132)$ PI-PLC $\delta 1$; ($\bigcirc$) full-length PI-PLC $\delta 1$. Assay conditions were the same as in Figure 5 with 3 μg of full-length PI-PLC $\delta 1$ and 6 μg of $\Delta(1-132)$ PI-PLC $\delta 1$ and 0.5 mM CaCl$_2$.

follow Arrhenius' law (Douzou, 1971). Several enzymes have recently been analyzed by Arrhenius' law (Craig et al., 1996) and transition state theory (Mondal & Mitra, 1994; Arnold & Ulbrich-Hofmann, 1997). Both full-length and PH domain truncated PI-PLC $\delta 1$ were completely inactivated if the assay temperature was above 60 °C; hence, initial rates of activity toward PI were determined from 24 to 55 °C for $\Delta(1-132)$ PI-PLC $\delta 1$ and at 24−45 °C for full-length PI-PLC $\delta 1$ (Figure 7A,B). The temperature profile showed very similar effects on the ratio of cIP/I-1-P for both enzymes

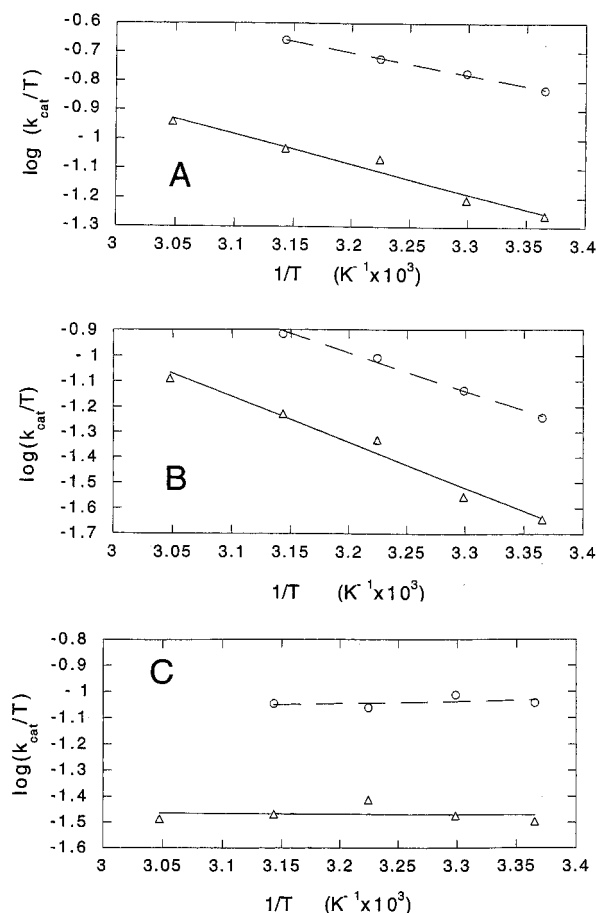FIGURE 8: Eyring plot of $\log(k_{cat}/T)$ versus $1/T$ for $\Delta(1-132)$ PI-PLC $\delta 1$ ($\triangle$) and full-length PI-PLC $\delta 1$ ($\bigcirc$) catalyzed hydrolysis of PI (A) to generate cIP (B) and I-1-P (C). The apparent activation enthalpies, $\Delta H^{\ddagger}$, for PI hydrolysis, cIP production, and the generation of I-1-P were determined by the slope of the plot to be 19.6, 34.0, and 0.0 kJ/mol, respectively, for the truncated enzyme, and 14.6, 28.5, and 0.0 kJ/mol, respectively, for the full-length clone.

(Figure 7C). Notable is the nearly temperature-independent generation of I-1-P while cIP production increased with increasing temperature. A plot of $\log(k/T)$, where k is the turnover number, versus $1/T$ for PI hydrolysis, cIP production, and the generation of I-1-P by the truncated and the full-length enzymes is shown in Figure 8.

An enzyme reaction is much more complicated than a simple elementary reaction where transition state theory holds. PI-PLC $\delta 1$ hydrolysis of PI is even more complicated because it involves many steps and two different products. The determination of a real $\Delta H^{\ddagger}$, $\Delta G^{\ddagger}$, and $\Delta S^{\ddagger}$ from the steady-state kinetics seems intractable. However, the linear relationship between $\log(k/T)$ and $1/T$ as shown in the Eyring plot (Figure 8) should allow us to determine an apparent $\Delta H^{\ddagger}$, $\Delta G^{\ddagger}$, and $\Delta S^{\ddagger}$. These values could shed some light on the PI-PLC $\delta 1$ mechanism. From the Eyring plots, the apparent activation enthalpies, $\Delta H^{\ddagger}$, for PI hydrolysis, cIP production, and the generation of I-1-P were determined to be 19.6, 34.0, and 0.0 kJ/mol, respectively, for the truncated enzyme, and 14.6, 28.5, and 0.0 kJ/mol, respectively, for the full-length clone. The experimentally determined apparent $\Delta H^{\ddagger}$, $\Delta G^{\ddagger}$, and $\Delta S^{\ddagger}$ values are summarized in Table 5 for the truncated enzyme and in Table 6 for the full-length enzyme. Notable is the high apparent $\Delta G^{\ddagger}$ (in the range of 63−74 kJ/mol), which accounts for the relatively low activity of PI-PLC $\delta 1$ toward PI; this $\Delta G^{\ddagger}$ is dominated by the

Table 5: Kinetic Activation Parameters for $\Delta(1-132)$ PI-PLC $\delta 1$ Hydrolysis of Micellar PI[a]

temperature (°C)	hydrolysis of PI $\Delta G^{\ddagger}$ (kJ mol^{-1}) $\Delta S^{\ddagger}$ (J mol^{-1} K^{-1})	generation of cIP $\Delta G^{\ddagger}$ (kJ mol^{-1}) $\Delta S^{\ddagger}$ (J mol^{-1} K^{-1})	generation of I-1-P $\Delta G^{\ddagger}$ (kJ mol^{-1}) $\Delta S^{\ddagger}$ (J mol^{-1} K^{-1})
24	65.9	68.0	67.1
	−156	−114	−226
30	66.9	68.9	68.4
	−156	−115	−226
37	67.6	69.2	69.7
	−155	−113	−225
45	69.2	70.3	71.8
	−156	−114	−226
55	70.7	71.7	74.2
	−156	−115	−226

[a] $\Delta H^{\ddagger}$ was determined from the slope of Figure 8 as 19.6, 34.0, and 0.0 kJ mol^{-1} for the hydrolysis of PI, the generation of cIP, and I-1-P production, respectively.

Table 6: Kinetic Parameters for Full-Length PI-PLC $\delta 1$ Hydrolysis of Micellar PI

temperature (°C)	hydrolysis of PI $\Delta G^{\ddagger}$ (kJ mol^{-1}) $\Delta S^{\ddagger}$ (J mol^{-1} K^{-1})	generation of cIP $\Delta G^{\ddagger}$ (kJ mol^{-1}) $\Delta S^{\ddagger}$ (J mol^{-1} K^{-1})	generation of I-1-P $\Delta G^{\ddagger}$ (kJ mol^{-1}) $\Delta S^{\ddagger}$ (J mol^{-1} K^{-1})
24	62.9	65.8	64.6
	−163	−125	−218
30	64.4	66.5	65.8
	−164	−125	−217
37	65.6	67.3	67.6
	−164	−123	−218
45	66.9	68.4	69.2
	−164	−125	−218

[a] $\Delta H^{\ddagger}$ was determined from the slope of Figure 9 as 14.6, 28.5, and 0.0 kJ mol^{-1} for the hydrolysis of PI, the generation of cIP, and I-1-P production, respectively.

negative apparent activation entropy $\Delta S^{\ddagger}$. The apparent activation entropy, $\Delta S^{\ddagger}$, values for PI hydrolysis, release of cIP, and the generation of I-1-P were similar for both full-length and truncated enzymes and estimated as −160, −120, and −220 J mol^{-1} K^{-1}. The higher activation entropy for I-1-P production versus cIP release presumably reflects the energetic cost for ordering a water molecule to attack the bound cIP.

DISCUSSION

cIP Kinetics: How Can a Monomeric Enzyme Display Cooperative Kinetics? The observation that cIP is a substrate, although not a very good one, for PI-PLC $\delta 1$ is consistent with a sequential mechanism for PI hydrolysis. cIP hydrolysis is characterized by a high apparent K_m, low V_{max}, and notable cooperativity in cIP saturation curve. A comparison of the $\Delta(1-132)$ PI-PLC $\delta 1$ phosphotransferase activity for PI (16 μmol min^{-1} mg^{-1}) to the cyclic phosphodiesterase activity toward cIP (0.39 μmol min^{-1} mg^{-1}) indicates a significant enhancement in catalytic activity for PI cleavage. The enhancement becomes even more pronounced if one includes the difference in substrate K_m values. The K_m for the cIP hydrolysis reaction (25 mM) is considerably larger than the estimates for PI cleavage [the range for an apparent K_m is 20 μM to 1 mM for the bacterial PI-PLC (Zhou et al., 1997)]. This strongly suggests that the lipophilic portion of the substrate greatly enhances the catalysis. A clue to what is occurring may be provided by the observation that cIP hydrolysis displays cooperative saturation behavior. Since the conformation of the water-soluble substrate does

not change with increasing concentration in solution, the sigmoidal kinetics of cIP hydrolysis must be related to an effect of cIP on the enzyme that partially switches it from a less active to a more active form. The cooperativity in cIP kinetics could be explained by multiple binding sites for cIP (one at the active site, another at a site where its binding enhances catalysis), enzyme dimerization, or other conformational changes that perturb the active site including active site hydration (Wu & Roberts, 1997). The X-ray crystal structure suggested that PI-PLC $\delta 1$ is a monomeric enzyme with one active site (Essen et al., 1996). Gel filtration failed to detect any significant dimerization in the absence of substrate (R. L. Williams, unpublished results). Therefore, it is very unlikely that the cooperativity observed for both the full-length and the PH domain truncated enzyme hydrolysis of cIP is generated by site−site interactions, especially when taking into account that the cooperativity is persistent and independent of assay conditions (i.e., addition of diC$_7$PC micelles or organic solvents). If an enzyme dimer, induced by substrate, is the active form of the enzyme, then it must be transient for soluble substrates. The possibility of a second cIP site is intriguing since the cooperativity of the enzyme is abolished when phosphorylated GPIP$_x$ is the substrate. Clearly, the enzyme has a site with a strong affinity for phosphates. It is possible that as the cIP concentration is increased, the cIP phosphate moiety binds to the enzyme side chains that normally interact with the 4′-phosphate in such a fashion as to alter the conformation of the cIP already bound in the active site.

Other types of enzyme conformational changes might be involved in the transition from less active to more active forms. Recent NMR studies on PLA$_2$ have shown small conformational changes that primarily involve decreased flexibility in the active site when the enzyme is bound to an interface as well as a substrate analog. Only in the presence of an interface and a substrate analog is the conformational change accomplished (Petters et al., 1992; Van den Berg et al., 1995). A similar change may be happening for PI-PLC $\delta 1$. A comparison between the structures of the active sites of free and substrate analogue-complexed PI-PLC $\delta 1$ suggests that there are very few differences in the active site brought about by substrate binding. Only Glu 341 and Arg 549 move significantly upon binding substrate. The side chains of these residues move so that the Arg 549 makes closer interaction with the 4-phosphoryl group of the bound substrate. A possible alternate candidate for the conformational switch might be the X/Y linker sequence (residues 443−488) that is disordered in the crystal structure. It may be that this sequence is able to influence substrate entrance or product exit from the active site. The much larger X/Y linker of PLC-γ has been shown to act as an inhibitor of the enzyme (Horstman et al., 1996).

Interfacial Activation and Organic Solvent Activation. Interfacial activation, the enhancement of k_{cat} by enzyme binding to an interface, is a common feature for phospholipases. Mechanisms for this activation include substrate-based (such as changes in the conformation or surface concentration of substrates) and enzyme-based (changes in the conformation or enzyme dimerization or allosteric binding etc.) effects. These effects are difficult to separate with an aggregated substrate. Using a water-soluble substrate such as cIP that has no tendency to aggregate has proved to be useful in understanding the interfacial activation mech-

anism for bacterial PI-PLC (Zhou et al., 1997). In that case, interfaces are allosteric activators of the enzyme. Water-miscible organic solvents such as isopropyl alcohol, DMF, and DMSO can also activate bacterial PI-PLC hydrolysis of cIP by mimicking the polarity of the interface (Wu & Roberts, 1997). Both of these effects are types of interfacial activation different from what is usually associated with phospholipases. Similar activation phenomena occur with rat PI-PLC $\delta 1$. DMSO causes a 4-fold increase in V_{max} for both PI-PLC $\delta 1$ and the bacterial enzyme, suggesting that the effect of solvent on the catalytic step is similar for both of these enzymes. This has been postulated to involve partially dehydrating substrate and active site in the case of the bacterial PI-PLC (Wu & Roberts, 1997). Anchoring the enzyme to a phospholipid interface may likewise affect the hydration environment of the active site since this is not a buried active site but one relatively well exposed to solvent (Essen et al., 1996, 1997). The interfacial activation induced by PC had a much more pronounced effect on the bacterial enzyme, increasing $V_{max} \sim$ 7-fold, decreasing $K_m \sim$ 3-fold, and abolishing the cooperativity seen in the cIP saturation curve. For PI-PLC $\delta 1$, PC only increased V_{max} with no effect on substrate binding. Furthermore, the enhancement was only observed if the PH domain was intact. In both these enzymes, a phospholipid interface clearly has an allosteric role in enzyme activity. A likely explanation is that in aqueous solution there is an equilibrium between less active and more active forms of the enzyme. Both PC interfaces (by interacting with the PH domain) and organic solvent effectors modulate PI-PLC $\delta 1$ by changing the equilibrium between these two forms of the enzyme.

The PH Domain of PI-PLC $\delta 1$ Has an Allosteric Role. Mammalian PI-PLC contains two domains, PH and C2, that are thought to be important for membrane binding in many proteins. In the specific case of PI-PLC $\delta 1$, the crystal structure led to a 'tether and fix' model for membrane binding (Essen et al., 1996). In that model, the PH domain of PI-PLC $\delta 1$ tethers the enzyme to the membrane by specific binding to PIP$_2$, and the C2 domain fixes the catalytic domain in a productive orientation relative to the membrane. The PH domain of PI-PLC $\delta 1$ has been shown to bind PIP$_2$ with high affinity (Yagisawa et al., 1994; Lemmon et al., 1995; Garcia et al., 1995). PIP$_2$ binding to the PH domain affects the catalytic activity of PI-PLC $\delta 1$, enabling the processive hydrolysis of membrane-bound substrates (Cifuentes et al., 1993; Lomasney et al., 1996).

Kinetic constants (Table 1) for PI-PLC $\delta 1$ hydrolysis of water-soluble cIP in the absence and presence of an interface show that the PH domain truncated enzyme cannot be activated by the presence of a PC interface. Clearly, it is the PH domain that accounts for this interfacial activation for mammalian PI-PLCs. Although diC$_7$PC micelles provide a very effective interface for the activation of bacterial PI-PLC, they may not be optimal for the mammalian enzymes (PIP$_2$ cannot be used because it would be a much better substrate than cIP). While the micellar diC$_7$PC activation is controlled by the PH domain, it cannot be due to tethering the enzyme to a substrate-rich interface, because cIP is a water-soluble substrate.

Interestingly, the full-length enzyme is about 2-fold more active than the truncated one toward PI hydrolysis in Triton X-100 mixed micelles. This suggests that the PI/Triton X-100 micelle system induces the same conformational

change of PI-PLC $\delta 1$ as the allosteric interfacial activation by PC micelles. Since the $\Delta(1-132)$ PI-PLC $\delta 1$ enzyme still has an intact C2 domain, that entity alone is not sufficient for optimal activity. The C2 domain may still bind to an appropriate phospholipid interface, but this does not cause the allosteric changes that modulate k_{cat}.

Phosphorylated Water-Soluble Substrates: An Alternate Way To Access a High-Activity Form of PI-PLC $\delta 1$. The water-soluble GPIP$_x$ series provide a way to assess how inositol ring phosphorylation affects the phosphotransferase activity of PI-PLC $\delta 1$. GPI is such a poor substrate for the enzyme that it is hard to measure kinetic parameters accurately. V_{max}/K_m, as a measure of $\Delta(1-132)$ PI-PLC $\delta 1$ enzyme efficiency, is 0.016 for cIP; the value for GPI must be considerably less than that. The addition of the 4′-phosphate dramatically enhanced V_{max}, to a value roughly twice that for cIP, and reduced K_m to 1.8 mM, far below the value of 25 mM observed for cIP. Perhaps most interestingly, the presence of this phosphate on the inositol ring abolished the cooperativity observed in the cIP saturation curve. In terms of enzyme efficiency, this represents a 28-fold increase over cIP. This indicates the importance of 4′-phosphate for both substrate recognition and catalysis. The further addition of the 5′-phosphate had a pronounced effect on V_{max} (6-fold increase compared to cIP); K_m was increased to 2.6-fold that for GPIP, and, like GPIP, the dependence of activity on substrate concentration was hyperbolic. For GPIP$_2$ hydrolysis by $\Delta(1-132)$ PI-PLC $\delta 1$, the enzyme efficiency is 1.09. This was the maximal value observed for soluble substrates. All these observations are consistent with the crystallographic studies of $\Delta(1-132)$ PI-PLC $\delta 1$ complex with IP$_3$ (Essen et al., 1996, 1997) which showed that the 4′-phosphoryl group had the lowest *B*-factor (34 Å), indicating the lowest degree of structural disorder in the active site. This was followed by the 1′-phosphoryl group (40 Å) and the 5′-phosphoryl group (49 Å). The 4′-phosphoryl group has at least three direct hydrogen bonds with the enzyme involving Lys 438, Ser 522, and Arg 549. In addition, several indirect interactions with the enzyme are mediated by three intervening water molecules. These interactions could be critical both in aligning substrate and in converting the enzyme to its activated form. In contrast to the buried 4′-phosphoryl group, the exposed 5′-phosphoryl group forms only one salt bridge with Lys 440 and two water-mediated interactions.

A Sequential Mechanism with Comparable Release of cIP and Hydrolysis to I-1-P. cIP is such a poor substrate for the enzyme that it should be the major product if E·cIP and free cIP are in equilibrium when PI is hydrolyzed by PI-PLC $\delta 1$. The observation that mammalian PI-PLC enzymes generate both cyclic and acyclic inositol phosphates simultaneously (and in a fixed ratio) adds an important constraint to a simple sequential mechanism for PI hydrolysis. Structural studies of PI-PLC $\delta 1$ led to the speculation that PI was hydrolyzed by PI-PLC $\delta 1$ in a sequential mechanism but with slow release of cIP (Essen et al., 1997). This constraint is consistent with the difference in cIP hydrolysis kinetics when cIP is the substrate versus when PI is the substrate for the enzyme. Release of cIP produced *in situ* by the enzyme must be slow and comparable to the attack by a water molecule to produce I-1-P.

Given the cooperative kinetics of the cyclophosphodiesterase activity, the significant increase in observed rates
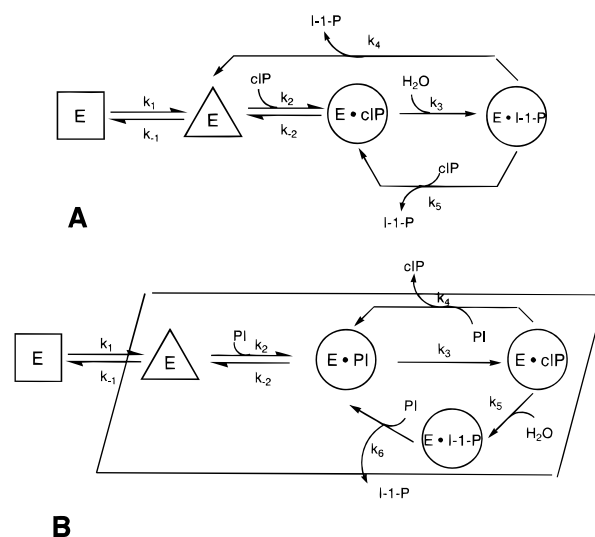

FIGURE 9: (A) Ligand-induced conformational change mechanism proposed for PI-PLC $\delta 1$ hydrolysis of cIP. The circle, the square, and the triangle represent the more active, the less active, and the partially active conformations, respectively. The switch from less active to partially activated form (k_1 step) can be achieved by the addition of an effective interface (i.e., diC$_7$PC), or a certain amount of water-miscible organic solvents (i.e., DMSO or iPrOH), or a ligand (i.e., cIP), or the combination of the above. cIP binding to the partially active enzyme (k_2 step) can further switch the enzyme to a more active state. At low cIP concentration, the release of the product, I-1-P (the k_4 step), is accompanied by the partial return of enzyme to a less active state. At high cIP concentration, the release of the product, I-1-P (the k_5 step), is accompanied by the addition of a second cIP; therefore, the enzyme has a higher probability of being maintained in its active form for many cycles of catalysis. (B) Sequential mechanism proposed for PI hydrolysis by PI-PLC $\delta 1$ is based on the formation of E·cIP as an intermediate with the release of cIP and attack of a water molecule in parallel reactions from this intermediate. The relative rates of step 4 (cIP release from the enzyme active site, which can be accelerated by a second PI binding) and step 5 (an activated water molecule attack on the E·cIP complex) control the ratio of cIP/I-1-P.

for PI hydrolysis, the fixed ratio of cIP/I-1-P at a given temperature, and the values of the apparent activation free energy, enthalpy, and entropy determined for PI hydrolysis based on the transition state theory (Figure 8), we can present a detailed scheme for the action of PI-PLC (Figure 9). In this model, PI-PLC $\delta 1$ exists in two major different states or conformations: a less active form (square) and a more active form (circle). In the absence of a ligand, the less active form is dominant. The presence of an effective interface or certain amount of water-miscible organic solvent can switch the enzyme to the partially active form (triangle), a metastable state between the most active and least active forms. Binding of substrates switches the distribution of enzyme toward the more active form (Figure 9A,B). Figure 9A is the scheme proposed for PI-PLC hydrolysis of water-soluble substrates such as cIP, while Figure 9B is proposed for micellar substrates such as PI dispersed in TX-100.

A difference between the water-soluble (Figure 9A) and micellar (Figure 9B) substrates is that for the micellar substrate, the enzyme is working in the processive mode [for recent reviews of processive mode kinetics, see Jain et al. (1995), Gelb et al. (1995), and Carman et al. (1995)]. When the enzyme is anchored to the interface, there is always a substrate molecule nearby ready to bind to the enzyme active site as soon as the product molecule is released. Furthermore, the binding to an interface may enhance the release
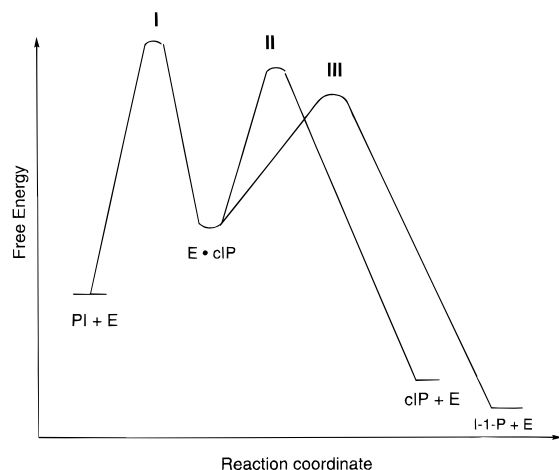
FIGURE 10: Energy landscape based on the experimentally determined apparent activation free energy and the sequential mechanism for PI-PLC $\delta 1$ hydrolysis of PI. The landscape is presented for the case that $K_m > $ [S] and $T = 24$ °C. At higher temperature, the transition state for cIP hydrolysis (labeled III) is at a higher energy than that for cIP release (labeled II); hence, the ratio of cIP/I-1-P increases.

of product molecule from the enzyme active site. The enzyme bound to the interface may also remain in its activated form. However, for water-soluble monomeric substrates such as cIP, a second cIP may not be able to bind to the enzyme active site soon enough after the release of product molecule I-1-P, to maintain the enzyme in its more active form, especially when the substrate concentration is low compared to the K_m (as is the case for cIP). In this case, the enzyme may relax back to its less active form (step 4). However, at high substrate concentration, a second substrate molecule may (i) have a better opportunity to bind to the more active form of the enzyme as soon as the product molecule is released, (ii) bind to an allosteric site, or (iii) enhance protein aggregation, any of which could produce observed cooperativity. The enzyme may remain in its activated form for many substrate turnovers (step 5). The observation that GPIP$_x$ substrates do not display cooperative kinetics can also be understood with this model. The extra phosphate on the 4-position of the inositol ring has strong interactions with the enzyme active site. This could stabilize the enzyme in its activated form even at low substrate concentrations.

For PI hydrolysis, initial steps (up through catalysis, step 3) to produce E·cIP are rate-determining. Release of free cIP (step 4) or hydrolysis to I-1-P (steps 5 and 6) represent alternative pathways for the intermediate E·cIP (Figure 10). As such, one expects the ratio of the two products (equivalent to the ratio of the rate constants for the two steps) to remain constant throughout the reaction progress curve at a given temperature. Altering the reaction temperature not only affects PI hydrolysis but also affects the ratio of cIP/I-1-P produced from E·cIP. The temperature dependence of the cIP/I-1-P ratio reflects the difference in $\Delta H^{\ddagger}$ for release of cIP versus hydrolysis to I-1-P (e.g., $\Delta\Delta H^{\ddagger}$). This is derived from

$$k_{cIP}/k_{I-1-P} = \exp[-(\Delta G^{\ddagger}_{cIP} - \Delta G^{\ddagger}_{I-1-P})/RT]$$

$$k_{cIP}/k_{I-1-P} = \exp[-(\Delta H^{\ddagger}_{cIP} - \Delta H^{\ddagger}_{I-1-P})/RT] \cdot \exp[(\Delta S^{\ddagger}_{cIP} - \Delta S^{\ddagger}_{I-1-P})/R]$$

or

$$k_{cIP}/k_{I-1-P} = \exp[-(\Delta\Delta H^{\ddagger})/RT] \cdot \exp[(\Delta\Delta S^{\ddagger})/R]$$

$\Delta\Delta H^{\ddagger}$ is $+30$ kJ/mol higher for release of cIP versus hydrolysis of cIP; however, the $\Delta\Delta S^{\ddagger}$ is $+0.1$ kJ/(K·mol) comparing cIP release versus hydrolysis. At room temperature, these two terms are comparable but cancel each other out in estimating $\Delta\Delta G^{\ddagger}$ (thus, equal amounts of cIP and I-1-P are produced). As T increases, $\Delta\Delta G^{\ddagger}$ becomes negative, favoring release of cIP compared to hydrolysis. Thus, the transition state theory analysis predicts that more cIP will be generated as the assay temperature increases.

The attack of an activated water molecule on the E·cIP complex includes moving one water molecule from the liquid state to the enzyme active site, which has an entropy cost of about 10 J mol^{-1} K^{-1} (Dunitz, 1994). The -55 J mol^{-1} K^{-1} difference in activation entropy for the generation of I-1-P versus overall PI hydrolysis could not be due simply to the removal of one water molecule from the bulk liquid phase to the enzyme active site. More likely, this represents the cooperative behavior of water molecules in the enzyme active site. Movement of one water molecule to the enzyme active site so that it can effectively attack the E·cIP complex could require many water molecules to adjust their positions.

These constraints on the sequential mechanism provide an explanation for the differential effects of agents that reduce water activity on PI-PLC-catalyzed production of cIP and I-1-P. Added NaCl had little effect on the overall PI hydrolysis but increased the cIP/I-1-P ratio. NaCl increases the dielectric constant, thereby weakening charge−charge interactions. Such interactions have been shown to be important for cICH$_2$P, a nonhydrolyzable cIP analog (Wu et al., 1997), binding at the active site of PI-PLC $\delta 1$ (Essen et al., 1997). Apparently, NaCl increases the rate of release of cIP but does not affect the transition state for hydrolysis of the cIP·E complex. In contrast to NaCl, addition of water-miscible organic solvents had pronounced effects on both the overall hydrolysis of PI and the cIP/I-1-P ratio. The organic solvents were more effective than an interface in switching the enzyme from the less active form to the more active form for cIP hydrolysis (Table 1). Organic solvents can decrease the dielectric constant of the assay medium and in this way enhance the charge interaction of cIP and PI-PLC. Organic solvent can lower the energy for the transition state for cIP·E hydrolysis more than it affects cIP release (alternatively, it could raise the activation energy for cIP release). Such effects would bias $\Delta\Delta G^{\ddagger}$ in favor of I-1-P production.

The observation that hydrolysis of PI in TX-100 micelles produced similar amounts of cyclic and acyclic products, while the hydrolysis of PIP in TX-100 micelles generated little cyclic product, can also be rationalized. The inositol 4'-phosphate group has multiple charge interactions with the enzyme (Essen et al., 1997) and could effectively lower the energy of the transition state for attack of water on E·cIP$_2$ to form IP$_2$ versus affecting the transition state for cIP$_2$ release. This phosphate group must be critical for switching the enzyme to its more active conformation, since the water-soluble GPIP$_x$ substrates exhibit hyperbolic kinetics with a high V_{max} compared to the nonphosphorylated water-soluble substrates.

Summary. For PI hydrolysis, the ratio of cIP/I-1-P is controlled by the difference in free energy for the transition states leading to release of cIP versus the attack of an activated water molecule on the E·cIP complex to produce I-1-P. The substrate saturation curve is sigmoidal for water-soluble substrates, such as cIP, with low affinity for the enzyme. However, the addition of a phosphate at the 4-position of glycerophosphoinositol dramatically enhances the affinity for the enzyme active site. The binding of the phosphorylated substrates also eliminates cooperative catalysis, possibly by shifting the equilibrium of the enzyme to a more active form.

REFERENCES

Arnold, U., & Ulbrich-Hofmann, R. (1997) *Biochemistry 36*, 2166−2172.

Bruzik, K. S., & Tsai, M. D. (1994) *Bioorg. Med. Chem. 2*, 49−72.

Bruzik, K. S., Moorish, A. M., John, D. Y., Rhee, S. G., & Tsai, M. D. (1992) *Biochemistry 31*, 5183−5193.

Bruzik, K. S., Guan, Z., Riddle, S., & Tsai, M. D. (1996) *J. Am. Chem. Soc. 118*, 7679−7688.

Cardenas, M. L., Rabajille, E., & Niemeyer, H. (1978) *Arch. Biochem. Biophys. 190*, 142−148.

Cardenas, M. L., Rabajille, E., & Niemeyer, H. (1984) *Eur. J. Biochem. 145*, 163−171.

Carman, G. M., Deems, R. A., & Dennis, E. A. (1995) *J. Biol. Chem. 270*, 18711−18714.

Cifuentes, M. E., Honkanen, L., & Rebecchi, M. J. (1993) *J. Biol. Chem. 268*, 11586−11593.

Colomo, M. F., & Bonilla-Rodriguez, G. O. (1996) *J. Biol. Chem. 271*, 4895−4899.

Craig, D. B., Arriaga, E. A., Wang, J. C. Y., Lu, H., & Dovichi, N. J. (1996) *J. Am. Chem. Soc. 118*, 5245−5253.

Douzou, P. (1971) *Biochimie 53*, 1135−1145.

Dunitz, J. D. (1994) *Science 264*, 670.

Ellis, M. V., Carne, A., & Katan, M. (1993) *Eur. J. Biochem. 213*, 339−347.

Essen, L.-O., Perisic, O., Cheung, R., Katan, M., & Williams, R. L. (1996) *Nature 380*, 595−602.

Essen, L.-O., Perisic, O., Katan, M., Wu, Y., Roberts, M. F., & Williams, R. L. (1997) *Biochemistry 36*, 1704−1718.

Eyring, H. (1935) *Chem. Rev. 17*, 65−77.

Ferguson, K. M., Lemmon, M. A., Schlessinger, J., & Sigler, P. B. (1995) *Cell 83*, 1037−1046.

Ferscht, A. (1985) *Enzyme Structure and Mechanism,* W. H. Freeman & Company, New York.

Garcia, P., Gupta, R., Shah, S., Morris, A. J., Rudge, S. A., Scarlata, S., Petrova, V., McLaughlin, S., & Rebecchi, M. J. (1995) *Biochemistry 34*, 16228−16234.

Gelb, M. H., Jain, M. K., Hanel, A. M., & Berg, O. G. (1995) *Ann.u Rev. Biochem. 64*, 653−688.

Heinz, D. W., Ryan, M., Bullock, T. L., & Griffth, O. H. (1995) *EMBO J. 14*, 3855−3863.

Horstman, D. A., Destefano, K., & Carpenter, G. (1996) *Proc. Natl. Acad. Sci. U.S.A. 93*, 7518−7521.

Jain, M. K., Gelb, M. H., Rogers, J., & Berg, O. G. (1995) *Methods Enzymol. 249*, 567−614.

Kim, J. W., Ryu, S. H., & Rhee, S. G. (1989) *Biochem. Biophys. Res. Commun. 163*, 177−182.

Lee, S. B., & Rhee, S. G. (1995) *Curr. Opin. Cell Biol. 7*, 183−189.

Lemmon, M. A., Ferguson, K. M., O'Brien, R., Sigler, P. B., & Schlessinger, J. (1995) *Proc. Natl. Acad. Sci. U.S.A. 92*, 10472−10476.

Lewis, K., Garigapati, V., Zhou, C., & Roberts, M. F. (1993) *Biochemistry 32*, 8836−8841.

Lomasney, J. W., Cheng, H.-F., Wang, L.-P., Kuan, Y.-S., Liu, S.-M., Fesik, S. W., & King, K. (1996) *J. Biol. Chem. 271*, 25316−25326.

Mondal, M. S., & Mitra, S. (1994) *Biochemistry 33*, 10305−10312.

Neet, K. E. (1995) *Methods Enzymol. 249*, 519−567.

Paterson, H. F., Savopoulos, J. W., Perisic, O., Cheung, R., Ellis, M. V., Williams, R. L., & Katan, M. (1995) *Biochem. J. 312*, 661−666.

Petters, A. R., Dekler, N., van den Berg, L., Boelens, R., Katein, R., Slotboom, A. J., & de Haas, G. H. (1992) *Biochemistry 31*, 10024−10030.

Rabin, B. R. (1967) *Biochem. J. 102*, 22−23c.

Rebecchi, M. J., Eberhardt, R., Delaney, T., Ali, S., & Bittman, R. (1993) *J. Biol. Chem. 268*, 1735−1741.

Rhee, S. G., & Choi, K. D. (1992) *J. Biol. Chem. 267*, 12393−12396.

Rhee, S. G., Suh, P.-G., Ryu, S.-H., & Lee, S. Y. (1989) *Science 244*, 546−550.

Roberts, M. F., Wu, Y., Zhou, C., Geng, D., & Tan, C. (1996) *Adv. Enzyme Reg*ul. *36*, 57−71.

Ryu, S. H., Suh, P.-G., Cho, K. S., Lee, K.-Y., & Rhee, S. G. (1987*) Proc. Natl. Acad. Sci. U.S.A. 84*, 6649−6653.

Seitz, S. P., Kaltenbach, R. F., Vreekamp, R. H., Calabrese, J. C., & Perrela, F. W. (1992) *BioMed. Chem. Lett. 2*, 171−174.

Shashidhar, M. S., Volwerk, J. J., Keana, F. W., & Griffith, O. H. (1989) *Biochim. Biophys. Acta 1042*, 410−412.

Soltys, C., & Roberts, M. F. (1994) *Biochemistry 33*, 11608−11617.

Storer, A. C., & Cornish-Bowden, A. (1977) *Biochem. J. 165*, 61−69.

Suzuki, H., & Kanazawa, T. (1996) *J. Biol. Chem. 271*, 5481−5486.

Van den Berg, B., Tessari, M., de Haas, G. H., Verheij, H. M., Boelens, R., & Kaptein, R. (1995) *EMBO J. 14*, 4123−4131.

Volwerk, J. J., Shashidhar, M. S., Kuppe, A., & Griffith, O. H. (1990) *Biochemistry 29*, 8056−8062.

Wu, Y., & Roberts, M. F. (1997) *Biochemistry 36*, 8514−8521.

Wu, Y., Zhou, C., & Roberts, M. F. (1997) *Biochemistry 36*, 356−363.

Yagisawa, H., Hirata, M., Kanematsu, T., Watanabe, Y., Ozaki, S., Safuma, K., Tanaka, H., Yabuta, N., Kamata, H., Hirata, H., & Nojhima, H. (1994) *J. Biol.Chem. 269*, 20179−20188.

Zhou, C., Wu, Y., & Roberts, M. F. (1997) *Biochemistry 36*, 347−355.